JOURNAL OF APPLIED ELECTROCHEMISTRY 23 (1993) 38–43

Studies of space-averaged mass transport in the FM01–LC laboratory electrolyser

C. J. BROWN, D. PLETCHER

Department of Chemistry, University of Southampton, Southampton SO9 5NH, Great Britain

F. C. WALSH

Department of Chemistry, University of Portsmouth, Portsmouth PO1 2DT, Great Britain

J. K. HAMMOND, D. ROBINSON

ICI Chemicals & Polymers Ltd, Research and Development Department, P.O. Box 8, The Heath, Runcorn, Cheshire WA7 4QD, Great Britain

Received 23 January 1992; revised 2 May 1992; accepted 16 May 1992

Measurements of the mass transport limited current for the reduction of ferricyanide in 1 M potassium hydroxide and of copper(II) in 1.5 M sulphuric acid as a function of electrolyte flow rate are used to characterize the space-averaged mass transport properties of the FM01 laboratory electrolyser, with and without six types of polymer mesh turbulence promoters. In the absence of a promoter, the results followed the equation

$$Sh = 0.22\ Re^{0.71}\ Sc^{0.33} \qquad \text{for } 200 < Re < 1000$$

For the cell with the preferred turbulence promoter, the corresponding equation is

$$Sh = 0.74\ Re^{0.62}\ Sc^{0.33} \qquad \text{for } 200 < Re < 1000$$

Pressure drop data are also reported and it is confirmed that the presence of a turbulence promoter need not lead to a significant increase in the pressure drop over the reactor.

1. Introduction

The rates of many electrochemical processes are limited by the mass transport of the reactant to the electrode surface. Increasing the velocity of the electrolyte flow through a parallel plate cell reduces the thickness of the diffusion boundary layer and increases the rate of mass transport to the electrode. This leads to higher energy consumption for pumping, increased capital cost for pumps/pipework and a lower conversion per pass. An alternative approach to increasing the rate of mass transport is to insert an inert turbulence promoter in the path of the electrolyte. Since this need not increase pumping costs significantly and if the reaction is mass transport controlled, increases the conversion per pass, it is not surprising that turbulence promoters are widely employed in electrochemical technology.

Most commonly, mass transport is characterized by space averaged parameters estimated by measuring the limiting current under appropriate conditions [1–6]. Many authors [7–16] have investigated the effect of turbulence promoters considering factors such as the orientation, mesh size and electrolyte velocity. As well as increasing the mass transport, promoters can often give a more uniform current distribution [17, 18]. It is, however, important to determine the increase in the overall pressure drop due to the presence of the turbulence promoter [17] in the cell.

This paper reports the characterization of mass transport within a commercially available laboratory electrolyser, the FM01–LC supplied by ICI, and examines the effect of various turbulence promoters on the overall mass transport. Pressure drop measurements are also reported. A preliminary report [19] of this work has already appeared in a conference proceedings and an accompanying paper [20] reported some parallel studies in the commercial scale FM21–SP. An earlier paper [18] also described a technique for the investigation of local mass transfer within a cell and used the FM01–LC electrolyser to illustrate the experiments. As is the case with most industrial electrolysers, the FM01–LC is designed without entry and exit zones, and hence the mass transport regime must be expected to differ from that in cells used for many academic studies [7–11, 21].

2. Experimental details

2.1. *Flow cell and current measurement*

Details of the flow circuit [18] and electrochemical cell [18, 20, 22] are given in earlier publications. A potentiodynamic technique was used for this study. The potential of the working electrode was measured against a commercial SCE reference electrode (Radiometer type 401) and contact to the working electrode

0021-891X

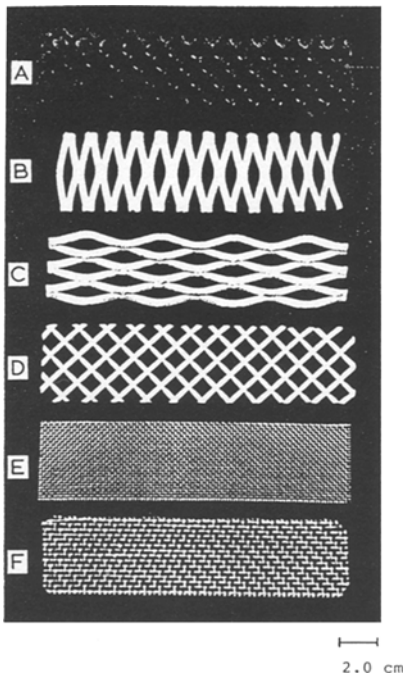

Fig. 1. Turbulence promoters used during the study. The characteristics of types A–F are shown in Table 1.

was through a Luggin capillary tube inserted into the channel wall of the spacer. The working electrode potential was controlled by a HiTek DT2101 potentiostat and PPR1 waveform generator, with current–potential curves being recorded on a Gould 60000 series chart recorder.

2.2 *Pressure drop measurement*

Pressure tappings were located (a) external to the cell within the electrolyte feed pipes to the inlet and from the outlet of the cell (b) within the cell electrolyte chamber as near as possible to the leading and trailing edges of the working electrode by drilling 1 mm holes through the cell spacer. Differential manometers employing either mercury or carbon tetrachloride were used depending on the magnitude of the pressure drop.

2.3. *Promoters and electrodes*

Six different turbulence promoters were used in this study (see Fig. 1 and Table 1). The FM01–LC electrolyser is constructed to give electrode dimensions of 16 cm (length) × 4 cm (height) and electrolyte flow is across the electrode; when set up in the undivided mode and the cell compressed to the recommended torque, the interelectrode gap is 0.55 cm. Hence, the cross sectional area of the empty channel is 2.20 cm^2. Each promoter had the overall dimensions, 16 cm × 4 cm so that they occupied the full length and height of the channel. Promoters A–D were 0.55 cm thick and a single sheet of the polymer, therefore, filled the channel completely. In the case of promoters E and F, a stack of the polymer nets, randomly superimposed, was used; the number of nets were chosen so that the promoters completely filled the channel when the cell was compressed according to the manufacturers recommendations. Throughout the paper, data are presented in terms of the nominal linear flow velocity.

For the copper experiments, both the anode and cathode were flat plate copper electrodes, active area 16 cm × 4 cm. Each electrode was prepared using 600 then 1200 grade emery paper before being washed with distilled water and degreased with acetone. For most of the ferricyanide experiments, nickel electrodes, active area 16 cm × 4 cm, were used. The initial pretreatment was the same as above but the cathode was then electrochemically cleaned by evolving hydrogen in 1 M potassium hydroxide at a current density of 10 mA cm^{-2} for 1200 s. Smaller nickel electrodes were prepared by blanking off the unwanted areas with a chemically resistant lacquer (Lacomit, supplied by W. Canning Materials Ltd).

2.4. *Experimental procedure*

The electrolytes used with the nickel electrodes consisted of either 2×10^{-3} M potassium ferricyanide plus 5×10^{-3} M potassium ferrocyanide, or 5×10^{-3} M potassium ferricyanide plus 12.5×10^{-3} M potassium ferrocyanide (solution A), both in 1 M potassium hydroxide (all BDH AnalaR). For the copper experiments, the electrolyte consisted of 7×10^{-3} M copper (II) sulphate in 1.5 M sulphuric acid (solution B). The physical properties of the two electrolyte solutions are listed in Table 2. Fresh solutions were used for each experiment. After the cell was assembled, the flow system was loaded with the electrolyte and purged with nitrogen for 20 min, with a continuous purge being maintained on the closed reservoir during the course of the experiment. Current against potential characteristics were recorded at a linear sweep rate of 3 mV s^{-1} for all the experiments, over a mean linear velocity range of 2.4 to 9.7 cm s^{-1}. Experiments were carried out at 298 K.

3. Results and discussion

3.1. *Mass transfer coefficients*

3.1.1. The ferricyanide system. Current against potential curves for the reduction of ferricyanide at the nickel cathode were recorded at a series of flow rates (both with and without turbulence promoters in the electrolyte flow) by scanning from the rest potential (+0.22 V) to −1.1 V/SCE at 3 mV s^{-1}. All the responses showed steeply increasing cathodic currents close to the equilibrium potential and well defined limiting current plateaux extending from −0.05 V to −0.9 V/SCE where the onset of hydrogen evolution is observed. The limiting currents were measured at the mid-point of these plateaux. Mass transfer coefficients, k_L, were then estimated using the equation

$$k_L = j_L/nFc \quad (1)$$

Table 1. Characteristics of the turbulence promoters

Promoter type	*Material*	*Number used*	*CD*/mm*	*LD†/mm*	*Orientation in direction of flow*	*Overall voidage‡*
A	blown polyethylene	1	7	9	LD	0.80
B	high density polyolefin	1	7	28	CD	0.84
C	high density polyolefin	1	7	28	LD	0.86
D	PTFE	1	11	11	N/A	0.83
E	polypropylene	8	1.0	1.0	N/A	0.63
F	polypropylene	5	1.7	1.7	N/A	0.57

* Internal dimension of short mesh diagonal.
† Internal dimension of long mesh diagonal.
‡ Ratio of free space in the channel to overall channel volume.

where j_L is the mass transport controlled current density (I_L/A) and c is the bulk concentration of ferricyanide. Each measurement was repeated five times and the values were averaged; the standard deviation was never greater than 5% for any data set.

Figure 2 shows the variations in k_L with the linear flow velocity of the electrolyte, v, for the cell with an empty channel together with the results obtained with the six turbulence promoters. The slope of the $\log k_L$ against $\log v$ plot for the empty channel was calculated to be 0.70 which is significantly higher than that with a promoter. The slopes were similar for all the promoters, values lying in the range 0.59 ± 0.02. The increase in mass transport coefficient achieved by the promoters is seen to vary from a factor of just under 1.7 for promoter C, to just over 3.8 for promoter E. Another point of interest is the performance offered by promoters B and C which only differ in their orientation to the electrolyte flow; promoter B with its short diagonal in the direction of fluid flow, increases the mass transfer coefficient by a factor of two greater than promoter C, the latter having the long diagonal in the direction of flow. This observation is consistent with earlier conclusions in the literature [9] and shows the importance of orientation when using promoters of this type. The results for the empty channel and for promoter A compare well with those reported by Robinson [22].

The results also highlight the importance in the design of a turbulence promoter of all its dimensions (e.g. strand width and shape, length of short diagonal, length of long diagonal). Promoters, types A–D can be regarded as bulk promoters, compared to types E and F which can be described as mesh promoters and have the lowest percentage open areas. The highest increase in mass transport coefficient was shown by promoter E, the smallest of the mesh promoters. However, it is interesting to note that the type B bulk promoter performed marginally better than the type F mesh promoter. It should be emphasised that the increase in current density does not arise solely from an increase in real linear flow rate due to the presence of the promoters (the overall voidages are listed in Table 1). Indeed, this is a small contribution. The major factor is the increase in turbulence at the electrode surface. This can also be seen in the work reported earlier [18] which examined the influence of the turbulence promoter characteristics on the distribution of local current densities within the cell. For example, the presence of a turbulence promoter had a strong influence on the current distribution both along and across the

Table 2. Physical properties for the solutions studied

Property	*Solution A**	*Solution B†*
Relative density, ρ	$1.050\,g\,cm^{-3}$	$1.096\,g\,cm^{-3}$
Dynamic viscosity, η	$0.0102\,g\,cm^{-1}\,s^{-1}$	$0.0119\,g\,cm^{-1}\,s^{-1}$
Schmidt number, $\eta/\rho D$	1562	2172
Diffusion coefficient, D	$6.2 \times 10^{-6}\,cm^2\,s^{-1}$ for $Fe(CN)_6^{3-}$	$5.0 \times 10^{-6}\,cm^2\,s^{-1}$ for Cu(II)

* Solution A: 5×10^{-3} M potassium ferricyanide, 12.5×10^{-3} M potassium ferrocyanide in aqueous 1 M KOH.
† Solution B: 5×10^{-3} M copper (II) sulphate in aqueous 1.5 M H_2SO_4.

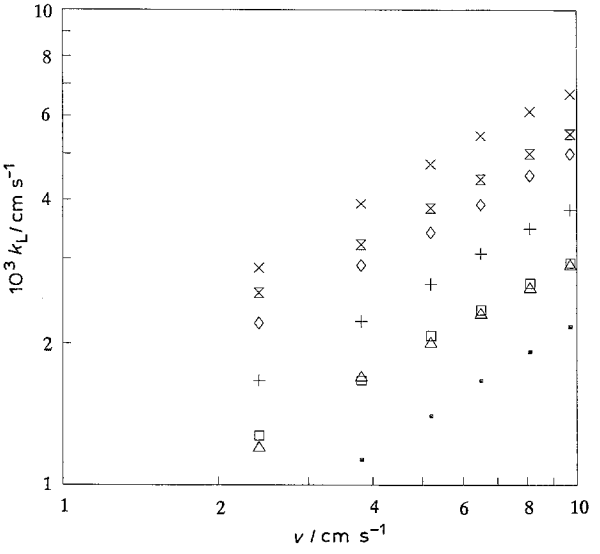

Fig. 2. Plots of $\log k_L$, against $\log v$ for the reduction of ferricyanide at a nickel electrode in the FM01 electrolyser with and without turbulence promoters. The electrolyte was 5×10^{-3} M potassium ferricyanide and 12.5×10^{-3} M potassium ferrocyanide in deoxygenated, aqueous 1 M KOH (solution A). $T = 298$ K. (●) no promoter and turbulence promoter: (+) type A, (⧖) type B, (□) type C, (△) type D, (×) type E, (◇) type F.

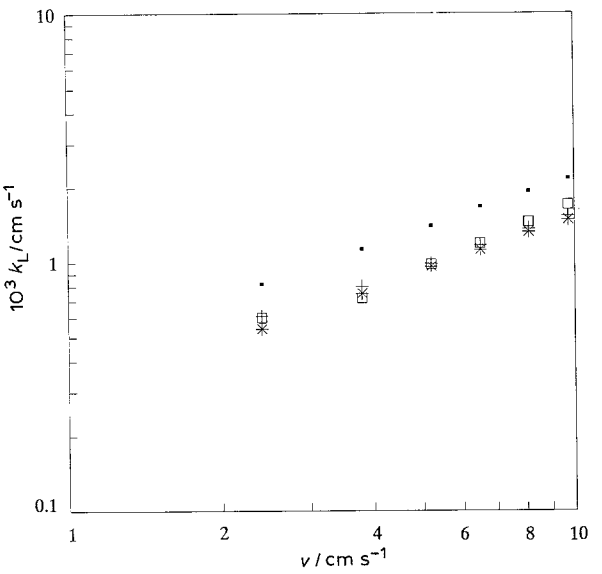

Fig. 3. Double logarithmic plot of the mass transport coefficient, k_L, against linear electrolyte flow velocity, v, for a series of different length entry and exit zones: (●) 0, (+) 2.5, (★) 5 and (□) 7.5 cm. Solution and conditions as Fig. 2.

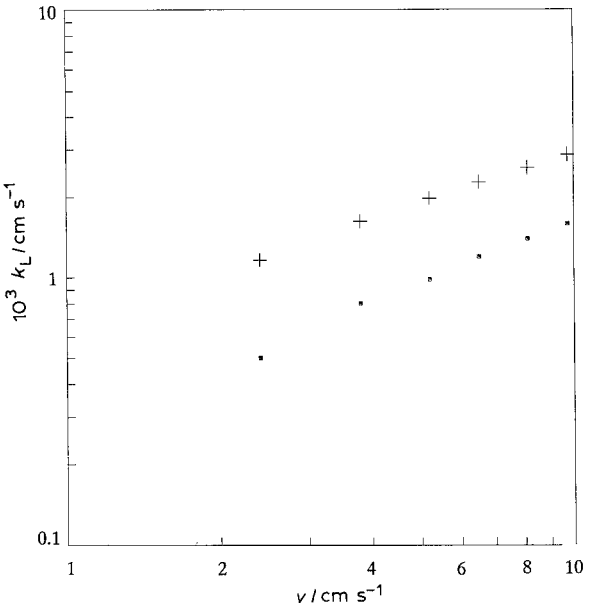

Fig. 4. Double logarithmic plot of the mass transport coefficient, k_L, against linear flow velocity for a flat plate copper electrode in a nitrogen purged solution of 7×10^{-3} M Cu^{2+} and 1.5 M H_2SO_4 (solution B) in the FM01 electrolyser. $T = 298$ K. (●) Empty channel, (+) type A promoter.

direction of electrolyte flow. These results and others reported in the literature [9–15] stress the fact that many of the characteristic dimensions of the promoters influence their performance. The relative values of the mass transfer coefficient will, however, also depend on the cell design [9, 16]. Hence, it is almost impossible to predict theoretically the optimum design of turbulence promoter for any cell.

3.1.2. The ferricyanide system with reduced area electrodes. It was considered of interest to investigate the influence of operating the cell with various entry and exit lengths. Hence, a series of experiments was performed with an open channel but with nickel electrodes, where the active area was restricted to the centre of the cell. Equal lengths of the electrode at the entrance and exit were blocked off with an insulating lacquer to create electrodes with lengths of 11, 6, and 1 cm (i.e. entry and exit zones each of lengths 2.5 cm, 5 cm and 7.5 cm respectively).

Figure 3 shows the mass transfer coefficient against flow rate plots for each of these electrodes and the data for the cell without entry and exit lengths is again shown for comparison. The data show that increased entry and exit zones result in a lower average rate of mass transport of reactant to the active electrode surface. This is to be expected due to the probable turbulent fluid flow regime at the inlet which results from the 'jet streams' flowing out from the electrolyte inlets in the internal manifolding [18]. To a lesser extent, there is also some turbulence at the outlet manifold. Apparently, inlet/outlet zones of 2.5 cm are sufficient to quieten the disturbances at the entry and exit of the cell since the results for all three electrodes of reduced size are very similar. It should also be noted that, perhaps more surprisingly, the introduction of entry/exit lengths does not cause a significant change to the slopes of the $\log k_L$ against $\log v$ plots.

3.1.3. The copper(II) system. These experiments employed a cell with a copper cathode both with an empty channel and with a type A turbulence promoter. The electrolyte was 7 mM copper(II) in 1.5 M sulphuric acid (solution B). Polarization curves were recorded by scanning the potential from the rest value to -0.5 V/SCE at 3 mV s^{-1}. Well defined limiting currents were obtained over a potential range of 300 mV. The variation in the mass transport coefficients with linear velocity for the copper electrode are shown in Fig. 4. The slopes of these plots, as well as the increase in k_L resulting from the type A turbulence promoter, are very similar to those reported above for the ferricyanide experiments.

3.2. *Dimensionless mass transport correlations*

Comparison of the mass transfer coefficients in Figs 2 and 4 show a significant difference between the two systems studied; the copper system gives lower mass transfer coefficients for both the promoted and unpromoted channel. As expected, however, the velocity exponents are similar in both cases. Hence, the data were recast into dimensionless group correlations which take into account the physical properties of the solutions.

Dimensionless group correlations were calculated in the form

$$Sh = a\, Re^b\, Sc^{1/3} \tag{2}$$

with the Sherwood number being defined by

$$Sh = k_L d_e / D \tag{3}$$

and the Reynolds number as

$$Re = v\, d_e / \nu \tag{4}$$

The hydraulic diameter of the cell, d_e, is calculated

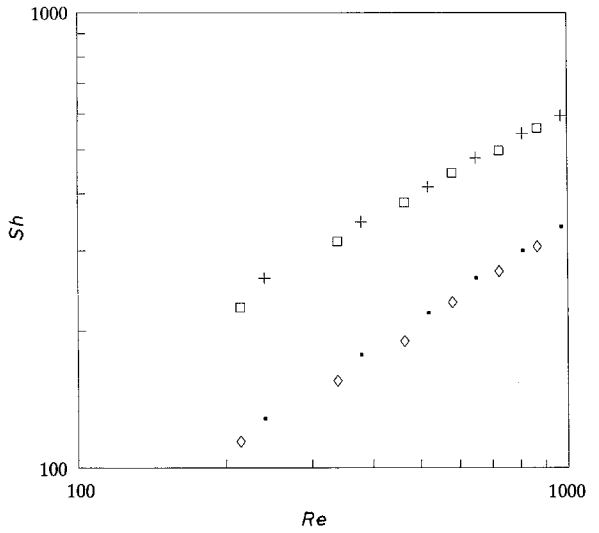

Fig. 5. Double logarithmic plot of the Sherwood against Reynolds number comparing the results for the two solutions studied. Solution A: (●) empty channel, (+) with turbulence promoter, type A. Solution B: (◇) empty channel, (□) with turbulence promoter, type A.

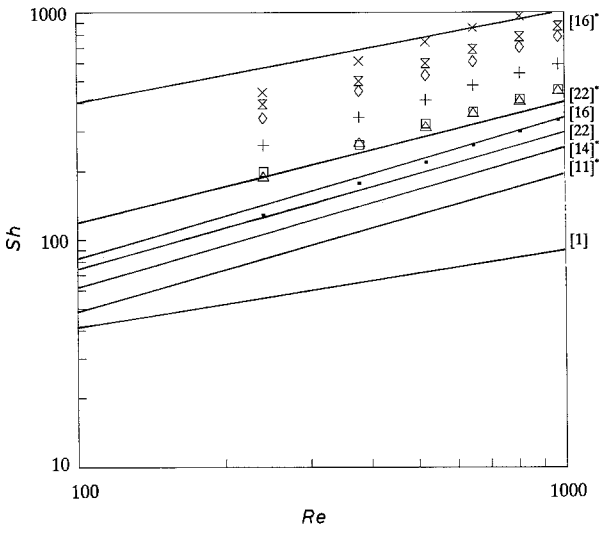

Fig. 6. Double logarithmic plots of the Sherwood against Reynolds number for the FM01 electrolyser with flat plate nickel electrode and using solution A. Also shown, for comparison, are literature data for other parallel plate cells with and without turbulence promoters (data from cells with promoter are marked *); literature references are shown. (●) No promoter and turbulence promoter: (+) type A, (×) type B, (□ type C, (△) type D, (×) type E and (◇) type F.

from

$$d_e = 2\,B\,S/(B + S) \quad (5)$$

where B is the height of the electrodes and S their separation. This gives the value $d_e = 0.97$ cm for the FM01-LC electrolyser. The diffusion coefficients, D, densities, ρ, and viscosities, ν, were each measured and the values obtained are reported in Table 2. The exponent for the Schmidt number was assumed to be 0.33.

The plots of log Sh against log Re are shown in Fig. 5. It can be seen that the data for the copper(II) solution and the ferricyanide solution now fall on the same lines for both (a) the cell with an empty channel and (b) for the cell with a turbulence promoter, type A. When the same data are presented as an equation of the form as Expression 2, a small difference (< 10%) between the Cu^{2+} and $Fe(CN)_6^{3-}$ solutions results from the difference in Schmidt number. Best fit lines were calculated using all the data points. With the empty channel, this gives

$$Sh = 0.22\,Re^{0.71}\,Sc^{0.33} \quad (6)$$

and for the cell with turbulence promoter, the corresponding equation is

$$Sh = 0.74\,Re^{0.62}\,Sc^{0.33} \quad (7)$$

The use of two different solutions to confirm mass transfer correlations in a given reactor geometry has not been common and here the agreement to within 10% is most pleasing.

Figure 6 shows Sherwood number against Reynolds number plots for the FM01 cell with and without turbulence promoters together with data for six other parallel plate cells, taken from the literature. It can be seen that the FM01 electrolyser compares favourably with most other cells. For the range of Reynolds number studied, $200 < Re < 1000$, the flow in an empty rectangular channel would be expected to be laminar and, hence to give a log Sh against log Re plot with a slope close to 0.3 as discussed in [1]. Figure 6 also shows the line with a slope 0.3 and it is obvious that all the practical cells give a slope which is markedly higher. In a cell incorporating internal manifolds and no calming section between the inlet and electrode face, however, a non-laminar flow regime would be expected giving the higher slopes observed. Indeed, flow visualization studies within the FM01 electrolyser [23] confirm the existence of turbulence at the inlet to the electrolyte chamber. This cannot, however, be the complete explanation since the introduction of inlet and outlet lengths to the cell did not lead to a reduction of the slope to 0.3.

3.3. *Pressure drop measurements*

The pressure drop was measured as a function of fluid flow velocity across the total cell (outlet and inlet manifolds and empty flow channel), using the pressure taps exterior to the cell, and the data are shown as a continuous line in Fig. 7. The pressure drop across the FM01 electrolyser is relatively high because of the restriction to flow imposed by the design of the electrolyte inlet and outlet.

Figure 7 also shows the pressure drop measurements for the empty flow channel and for the channel filled with the six turbulence promoters, determined using the pressure taps machined through the cell spacer. It can be seen that, although all the promoters lead to an increase in the pressure drop over that of the empty channel, only promoter E shows an increase comparable to that shown by the cell manifolds. Indeed, for the majority of the promoters, only a very small increase in the total pressure drop is observed. Similar results for a different cell using a plastic grid

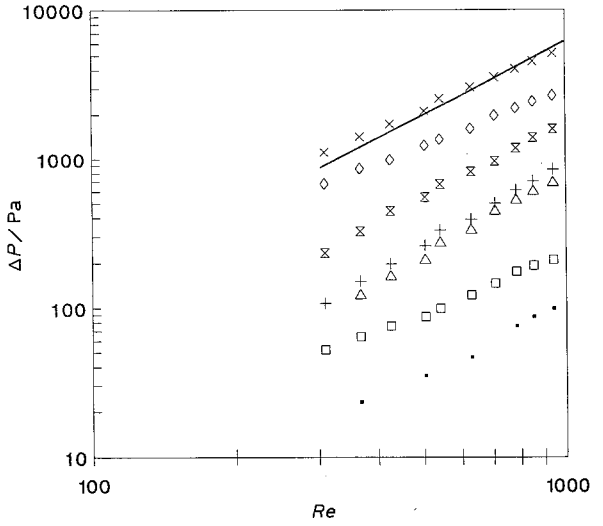

Fig. 7. Double logarithmic plot of the pressure drop against the Reynolds number for the FM01 electrolyser including inlet and outlet manifolds (shown as continuous line) and corresponding plots for the electrolyte chamber only, both empty and with the six turbulence promoters.

Turbulence promoter		$10^2 a/Pa$	b
None	●	0.69	1.39
type A	+	0.71	1.69
type B	⧖	1.82	1.65
type C	□	3.95	1.25
type D	△	1.69	1.54
type E	x	31	1.42
type F	◇	30	1.33
Total manifold	line	16	1.51

promoter has been noted in the literature [24]. Certainly, with the FM01 electrolyser, there is no significant increase in pumping costs resulting from the use of a turbulence promoter. The experimental data have been fitted to the equation

$$\Delta p = \mathbf{a}\, Re^b \qquad (8)$$

and the coefficients a and b are reported in the Table in the legend to Fig. 7.

Acknowledgement

The academic authors would like to thank ICI Chemical & Polymers Ltd for financial support of this programme.

References

[1] D. J. Pickett, 'Electrochemical Reactor Design', 2nd Edn, Elsevier, Amsterdam (1979).
[2] J. S. Newman, 'Electrochemical Systems', Prentice-Hall, Englewood Cliffs, New Jersey (1973).
[3] F. Coeuret and A. Storck, 'Eléments de Génie Electrochimique', Tecdoc, Paris (1984).
[4] D. Pletcher and F. C. Walsh, 'Industrial Electrochemistry', 2nd edn, Chapman & Hall, London (1990).
[5] A. A. Wragg, *Chem. Eng.* **316** (1977) 39.
[6] J. R. Selman and C. W. Tobias, *Adv. Chem. Eng.* **10** (1978) 211.
[7] F. B. Leitz and L. Marincic, *J. Appl. Electrochem.* **7** (1977) 473.
[8] M. M. Letord-Quéméré, J. Legrand and F. Coeuret, *IChemE Symposium Series* **98** (1986) 73.
[9] M. M. Letord-Quéméré and F. Coeuret, *J. Electrochem. Soc.* **135** (1988) 3063.
[10] W. W. Focke, *Electrochim. Acta* **28** (1983) 1137.
[11] F. Schwager, P. M. Robertson and N. Ibl, *ibid.* **25** (1980) 1655.
[12] A. T. Kuhn and R. W. Houghton, *ibid.* **19** (1974) 733.
[13] A. Storck and F. Coeuret, *ibid.* **22** (1977) 1155.
[14] V. Müller and I. Rousar, *Dechema Monograph* **123** (1991) 331.
[15] F. Leroux and F. Coeuret, *Electrochim. Acta* **30** (1985) 159.
[16] L. Carlsson, B. Sandegren and D. Simonsson, *J. Electrochem. Soc.* **130** (1983) 342.
[17] W. W. Focke, CSIR Report CENG 421, S. Africa (1982).
[18] C. J. Brown, D. Pletcher, F. C. Walsh, J. K. Hammond and D. Robinson, *J. Appl. Electrochem.*, **22** (1992) 613.
[19] C. J. Brown, D. Pletcher, F. C. Walsh, J. K. Hammond and D. Robinson, *Dechema Monographs* **123** (1991) 299.
[20] F. C. Walsh, J. K. Hammond and D. Robinson, *ibid.* **123** (1991) 317.
[21] A. Storck and D. Hutin, *Electrochim. Acta* **26** (1981) 127.
[22] D. Robinson, *in*: 'Electrosynthesis — From Laboratory, To Pilot, To Production', (edited by J. D. Genders and D. Pletcher), The Electrosynthesis Co., Buffalo NY (1990).
[23] C. J. Brown, D. Pletcher, F. C. Walsh, J. K. Hammond and D. Robinson, unpublished work.
[24] Ofelia de Queiroz Fernandes Araujo, MSc. Thesis, University of Illinois (1985).